NJC

PAPER

View Article Online
View Journal | View Issue

Cite this: *New J. Chem.*, 2017, 41, 6840

Amidoxime platinum(II) complexes: pH-dependent highly selective generation and cytotoxic activity†

Dmitrii S. Bolotin,*[a] Marina Ya. Demakova,[a] Anton A. Legin,[b] Vitaliy V. Suslonov,[c] Alexey A. Nazarov,[d] Michael A. Jakupec,*[b] Bernhard K. Keppler[b] and Vadim Yu. Kukushkin[a]

Received 24th March 2017,
Accepted 1st June 2017

DOI: 10.1039/c7nj00982h

rsc.li/njc

The reaction of *cis*-[$PtCl_2(Me_2SO)_2$] with 1 equiv. of each of the amidoximes $RC(NH_2)$═NOH in neutral media in MeOH results in the formation of complexes *cis*-[$PtCl_2${$RC(NH_2)$═NOH}(Me_2SO)] (5 examples; 83–98% isolated yields). In the presence of 2 equiv. of NaOH in MeOH solution, the reaction of *cis*-[$PtCl_2(Me_2SO)_2$] with 1 equiv. of each of the amidoximes $RC(NH_2)$═NOH leads to [Pt{RC(NH)═NO}$(Me_2SO)_2$] (7 examples; 74–95% isolated yields). All new complexes were characterized by C, H, and N elemental analyses, HRESI$^+$-MS, IR, ^{1}H, ^{13}C{^{1}H}, and CP-MAS TOSS ^{13}C{^{1}H} NMR spectroscopies, and additionally by single-crystal XRD (for seven species). The cytotoxic potency of six compounds was determined in the human cancer cell lines CH1/PA-1, A549, SK-BR-3, and SW480. Generally, the second class of complexes containing chelating amidoximato ligands shows much higher cytotoxicity than the non-chelate amidoxime analogs, despite the lack of easily exchangeable chlorido ligands. Especially, the complex [Pt(*p*-$CF_3C_6H_4$C(NH)═NO)$(Me_2SO)_2$] displays a remarkable activity in the inherently cisplatin resistant SW480 cell line (0.51 μM *vs.* 3.3 μM).

Introduction

Platinum-based anticancer drugs are among the most widely used chemotherapeutics and applied in the treatment of a wide range of malignant tumors.[1] Specifically in the treatment of testicular cancer, the introduction of cisplatin increased the survival rate to more than 90% of the diagnosed cases. The platinum chemotherapeutics cisplatin and the second and third generation compounds carboplatin and oxaliplatin, respectively, are now the first line of treatment for bladder, testicular, ovarian, head/neck and colorectal cancers.[2] However, severe toxic effects such as nausea, nephro- and neurotoxicity, and resistance of common cancer types to Pt compounds as well as resistance acquired during treatment limit their application to a great extent.[3]

The classic structure–activity relationships for platinum compounds are based on platinum being present as Pt^{II} or Pt^{IV} centers with two *cis*-configured leaving groups and two stable am(m)ine ligands coordinated to the metal.[4] While the complexes are supposed to remain in their original composition during administration and circulation in the bloodstream, the low chloride concentration in the cell allows a chlorido/aqua exchange to occur. Sequential replacement of the leaving ligands leads to positively charged complexes that interact initially electrostatically with the negatively charged phosphate backbone of DNA before a second step of ligand exchange reactions leading to the platination of DNA. Platinum is found most commonly attached to guanine residues in the major groove and to a lesser extent to adenine moieties. In particular, the presence of adjacent guanines residues has been found to be advantageous to support the binding event between the platinum center and DNA, leading to DNA lesions that cannot be repaired easily and trigger apoptosis.[5]

The nature of the leaving ligand(s) has been shown to be crucial for reducing the side effects, and this has especially been demonstrated for the second and third generation compounds, carboplatin and oxaliplatin, which feature the negatively charged cyclobutanedicarboxylato and oxalato ligands, respectively.[5c,6] However, there are also neutral ligands that can easily be substituted under physiological conditions. Ligands such as DMF and $(CH_3)_2SO$ have been widely used in the preparation of

[a] *Institute of Chemistry, Saint Petersburg State University, Universitetskaya Nab., 7/9, Saint Petersburg, Russian Federation. E-mail: d.s.bolotin@spbu.ru*
[b] *Institute of Inorganic Chemistry and Research Platform "Translational Cancer Therapy Research", University of Vienna, Währinger Strasse 42, A-1090 Vienna, Austria. E-mail: michael.jakupec@univie.ac.at*
[c] *Center for X-ray Diffraction Studies, Saint Petersburg State University, Universitetskii Pr., 26, Saint Petersburg, Russian Federation*
[d] *Department of Chemistry, Moscow State University, Leninskie Gory, 1,3, Moscow, Russian Federation*

† Electronic supplementary information (ESI) available: Characterization and spectra of **3a–b**, **3d–f**, and **4c–g**, X-ray structure determinations and crystal data of **3a–b**, **3d–f**, **4c**, **4f** and [**2cH**][$PtCl_3(Me_2SO)$], and concentration–effect curves of **3b**, **3d–e** and **4c–e**. CCDC 1475377, 1475378, 1475381, 1475389, 1475399, 1475400, 1475446 and 1475683. For ESI and crystallographic data in CIF or other electronic format see DOI: 10.1039/c7nj00982h

complexes and their metal species are often identified as intermediates.[6c,7] Furthermore, $(CH_3)_2SO$ is found in the ruthenium-based anticancer agent NAMI-A, which was studied for its antimetastatic effects in two clinical trials before being ruled out recently.[8]

More recently, interest has grown in the so-called rule-breaker compounds that do not follow the classic structure–activity relationships recognized for the established anticancer agents and their close analogs. Such rule-breakers are for example *trans*-configured Pt^{II} complexes, but also multinuclear platinum compounds have been investigated and the latter even reached clinical trials due to their potential to overcome cisplatin resistance at least in cell culture. Such non-classic compounds have been suggested to interact with DNA in a different manner from the platinum *cis*-complexes and thereby would have a different mode of action that may help to overcome the drawbacks of platinum-based chemotherapy.[9]

These considerations led us to the design and preparation of amidoxime and amidoximato Pt^{II} complexes. Oxime complexes have been shown in the past by us and others to exhibit anticancer activity in an *in vitro* setting.[10] Moreover, organic compounds featuring the amidoxime functional group have also been shown to be anticancer active.[11] The synthesis of the platinum complexes was performed starting from the platinum precursor *cis*-$[PtCl_2(Me_2SO)_2]$ and the amidoximes in methanol and in the presence of NaOH. Depending on the conditions, either the $[PtCl_2(\text{amidoxime-}\kappa^1\text{-}N_{oxime})(Me_2SO)]$ or the $[Pt(\text{amidoximato-}\kappa^2\text{-}O,N_{amide})(Me_2SO)_2]$ complexes were obtained. The cytotoxicity of three species of each class was screened in the human cancer cell lines CH1/PA-1, A549, SK-BR-3, and SW480, where the MTT assay revealed only marginal activity for the three amidoxime complexes, moderate activity for two of three amidoximato complexes, but a remarkably high cytotoxic potency for the complex bearing a *p*-trifluoromethylbenzamidoximate ligand, especially in the SW480 cell line. All our studies are consistently disclosed in sections that follow.

Results and discussion

Platinum(II) ketoxime complexes have been extensively studied for the last two decades and data related to these species indicated that ketoximes easily coordinate to the platinum(II) center by the N atom.[10d,12] Such platinum(II) complexes featuring *N*-bound oximes react with excess platinum(II) to obtain two- or trinuclear species featuring $\mu^2\text{-}\kappa^1\text{-}N\text{-}\kappa^1\text{-}O$ oxime ligands.[10b] In spite of that, amidoxime platinum(II) complexes are still remarkably less explored, whereas amidoxime complexes of other metals are studied as well as conventional oxime complexes.[13] Thus, only four platinum(II) complexes featuring amidoxime ligands are presented in the literature (Fig. 1).[14] Complexes **A** (*ca.* 100% yield) and **B** (50% yield) were obtained *via* the action of the corresponding amidoximes upon the binuclear complexes $[Pt(\mu_2\text{-}Cl)(SnCl_3)(PEt_3)]_2$ or $[Pt(\mu_2\text{-}Cl)(Ac)(C(Me)OH)]_2$, respectively. Complexes **C** (the cycle is phenyl or ferrocenyl; 25 and 18% yields) were obtained by the reaction of $RC(NH_2)$═NOH (R = Ph, Fc) with *cis*-$[PtCl_2(Me_2SO)_2]$ in MeOH upon reflux for 12–16 h.

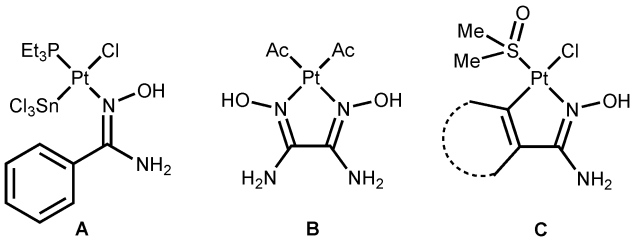

Fig. 1 Previously reported platinum(II) amidoxime complexes.

The four known amidoxime complexes feature exclusively N_{oxime}-ligated amidoximes and the NH_2 moiety of amidoxime ligands is unligated to the platinum(II) stipulating the amidoximes play a role of conventional oxime ligand. No examples of platinum(II) amidoxime complexes featuring the N_{amide}-bound ligands were previously reported. Moreover, as analysis of literature data indicated,[13] amidoxime species have at least four types of ligation in mononuclear complexes (Fig. 2) and the selective preparation of amidoxime complexes with an exact coordination mode is still an open problem.

The generation of type **II** complexes proceeds either with oxophilic metal centers or in the presence of a base due to the deprotonation of the O atom resulting in an increase of its nucleophilicity. The coordination of amidoximes by the O atom in basic media commonly is accompanied by the deprotonation of the NH_2 moiety with consequent chelation of the metal center giving type **IV** complexes. Type **III** complexes are mostly realized at electron-deficient metal centers, *viz.*, early transition metals or f-elements.

In this work, we decided to comprehensively investigate the preparation of amidoxime platinum(II) complexes with a particular purpose of finding selective routes for the generation of complexes with a well-defined coordination mode of amidoxime ligands. We planned the selective preparation of the complexes of types **I**, **II**, and **IV** by variation of the acidity of the reaction mixtures, whereas complexes of type **III** are hardly accessible at a rather electron-rich platinum(II) center. Previously, it was reported that the amidoxime OH group can be effectively deprotonated by NaOH in alcohol media[15] and, concurrently, amidoximes can be protonated at the oxime N atom by strong acids.[13] Because of these reasons, we decided to use NaOH and TfOH to vary the acidity of the reaction mixtures and to employ MeOH as a solvent.

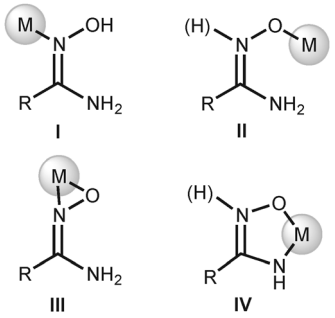

Fig. 2 Coordination modes of amidoximes in their mononuclear complexes.[13]

Synthesis and characterization of amidoxime complexes 3a–b and 3d–f

As the starting materials for this study, we addressed, on the one hand, *cis*-$[PtCl_2(Me_2SO)_2]$[16] (**1**) and, on the other hand, the aliphatic, aromatic, and heteroaromatic amidoximes $RC(NH_2)$═NOH (R = Me **2a**, Et **2b**, *t*-Bu **2c**, Ph **2d**, *p*-$CF_3C_6H_4$ **2e**, *p*-$O_2NC_6H_4$ **2f**, *p*-NC_5H_4 **2g**). The reaction of 1 equiv. of any one of the amidoximes **2a–b** or **2d–f** with complex **1** proceeds in MeOH at 65 °C for 5 min and results in the formation of amidoxime platinum(II) complexes **3a–b** or **3d–f** that were isolated in good to excellent yields (83–98%; Scheme 1a). The rate of this reaction is decreased by additions of TfOH (1 equiv.) and **3a–b** or **3d–f** forms for 1 h in 15–20% lower yields, which could be explained by simultaneous Tiemann rearrangement (for recent works, see ref. 17) of the amidoximes in the reaction mixtures (traces of corresponding ureas $RNHC(=O)NH_2$ were detected by ^{1}H NMR). Complexes **4a–g** (Scheme 1b) were not detected in the reaction mixtures by HRESI-MS and ^{1}H NMR.

Complexes **3a–b** and **3d–f** give satisfactory C, H, and N elemental analyses for the proposed formulas. These species were also characterized by HRESI$^+$-MS, IR, ^{1}H, $^{13}C\{^1H\}$, and CP-MAS TOSS $^{13}C\{^1H\}$ NMR spectroscopies, and additionally by X-ray diffraction (XRD). Compounds **3a–b** and **3d–f** are stable in the solid state at RT and upon heating decompose in the range of 142–185 °C.

A characteristic feature of the positive-mode high-resolution ESI mass spectra of **3a–b** and **3d–f** is the availability of sets of peaks related to fragmentation and quasi-ions corresponding to $[M - 2Cl + H]^+$, $[M - Cl]^+$, $[M - Cl - H + Na]^+$, $[M + Na]^+$, $[M + K]^+$, $[2M - 2Cl - 2H + Na]^+$, $[2M - Cl]^+$, $[2M + Na]^+$, $[2M + K]^+$, and $[3M - 2Cl - 2H + Na]^+$.

In the IR spectra of **3a–b** and **3d–f**, we observed two or three medium-strong to very strong bands in the region of 3480–3215 cm^{-1}, which can be attributed to the O–H and N–H stretches, and a set of weak to medium bands at 3187–2785 cm^{-1} assignable to the C–H stretches.[18] All spectra also display one very strong band in the 1663–1655 cm^{-1} region specific for the ν(C═N) of the amidoxime moiety[13] and one medium to very strong band at 1138–1105 cm^{-1} characteristic of the ν(S═O) stretches of sulfur-bound sulfoxides.[19] In addition, the spectrum of **3f** displays two very strong bands at 1520 and 1346 cm^{-1} specific for asymmetric and symmetric ν(N═O) bands of the NO_2 moiety.[18]

Complexes **3a–b** and **3d–f** are almost insoluble in the common deuterated organic solvents ($CDCl_3$, CD_2Cl_2, $(CD_3)_2CO$, and D_2O) apart from $(CD_3)_2SO$ and CD_3OD. In $(CD_3)_2SO$, the exchange of ligated $(CH_3)_2SO$ with the solvent molecules occurs for 5 min, and therefore the spectra were recorded in CD_3OD. A characteristic feature of the ^{1}H NMR spectra is the non-equivalence of the methyl groups of the Me_2SO ligand. Thus, the spectra of **3a–b** exhibit one unresolved broad singlet at 3.45 ppm (**3a**) or two singlets at 3.46 and 3.44 ppm (**3b**), whereas the spectra of **3d–f**, derived from aromatic amidoximes **2d–f**, display two singlets at 3.42–3.37 and 2.83–2.59 ppm. In **3d–f** relatively to **3a–b**, the high-field shift (0.59–0.78 ppm) of one of the methyl groups of the Me_2SO ligand should be associated with the shielding effect of the aromatic rings (see X-ray structure determinations).

The $^{13}C\{^1H\}$ NMR spectra in CD_3OD (**3a–b** and **3d–e**) exhibit a low-field signal at 162.29–157.89 ppm, which is attributed to the *C*═NOH carbon of the amidoxime moiety,[13] whereas in the high-field the spectra display two singlets attributed to the methyl groups of the Me_2SO ligand at 43.31–42.95 and 42.98–42.55 ppm, which agree well with the two singlets observed in the ^{1}H NMR spectra. Compound **3f** exhibits poor solubility in CD_3OD leading to a poor-quality $^{13}C\{^1H\}$ NMR spectrum even with long acquisition time and it was characterized by solid-state CP-MAS TOSS $^{13}C\{^1H\}$ NMR. The spectrum displays one singlet at 155.19 ppm from the C atom of the carbamidoxime moiety and four singlets of the methyl groups of Me_2SO ligand in the region of 46.59–40.18 ppm. Duplication of signals related to the Me_2SO ligand is probably due to two different conformations of **3f** in the solid sample.

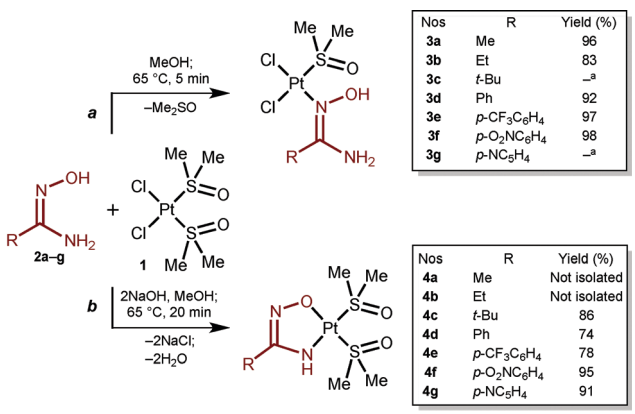

Nos	R	Yield (%)
3a	Me	96
3b	Et	83
3c	*t*-Bu	–[a]
3d	Ph	92
3e	*p*-$CF_3C_6H_4$	97
3f	*p*-$O_2NC_6H_4$	98
3g	*p*-NC_5H_4	–[a]

Nos	R	Yield (%)
4a	Me	Not isolated
4b	Et	Not isolated
4c	*t*-Bu	86
4d	Ph	74
4e	*p*-$CF_3C_6H_4$	78
4f	*p*-$O_2NC_6H_4$	95
4g	*p*-NC_5H_4	91

Scheme 1 Generation of amidoxime and amidoximate platinum(II) complexes. [a] Analytical data are not sufficient for full characterization.

Synthesis and characterization of amidoximate complexes 4a–g

The reaction of 1 equiv. of any one of the amidoximes **2a–g** with complex **1** in the presence of 2 equiv. of NaOH proceeds in MeOH at 65 °C for 20 min and leads to amidoximate platinum(II) chelated complexes **4a–g** (83–98%; Scheme 1b). Compounds **4a–b** were not separated from some by-products due to their similar solubilities in organic solvents and in H_2O and also because of decomposition of the mixture on silica gel. However, the formation of **4a** and **4b** was confirmed by HRESI$^+$-MS (**4a**: 424.0313 $[M + H]^+$, calcd 424.0323; **4b**: 438.0470 $[M + H]^+$, calcd 438.0480). Complexes **4a–g** form in a wide range of amidoxime and NaOH ratios. These complexes were isolated (for **4c–g**) from the reaction mixtures or detected in the mixtures (for **4a–b** see Fig. S26–S29, ESI†) when 1–10 equiv. of **2a–g** and 1–4 equiv. of NaOH were used. It was concluded that, on the one hand, the yields of **4c–g** do not significantly depend on the quantity of **2a–g** when it was taken in more than 1.1-fold excess. On the other hand, the yields gradually increase with increasing relative quantity of NaOH up to 2.5-fold excess. Upon further addition of the base, the yields decreased for 10–20% in the case to 4-fold excess of NaOH. In these experiments, the formation of the corresponding open-chain species **3** was not detected by HRESI-MS and ^{1}H NMR. Only when 0.1–2 equiv. of NaOH are

used, the reaction of **1** with **2** leads to mixtures of the corresponding complexes **3** and **4**.

Complexes **4c–g** give satisfactory C, H, and N elemental analyses for the proposed formulas. These species were also characterized by HRESI$^+$-MS, IR, ^{1}H, and ^{13}C{^{1}H} NMR spectroscopies, and additionally by XRD (for **4c** and **4f**). Compounds **4c–g** are stable in the solid state at RT and upon heating decompose in the range of 189–218 °C.

A characteristic feature of the positive-mode high-resolution ESI mass spectra of **4c–g** is the availability of sets of peaks related to fragmentation $[M - Me_2SO + H]^+$ (**4e**) and the quasi-ions $[M + H]^+$ and $[M + Na]^+$. The availability of a high-intensity set of peaks from $[M + H]^+$, which was not observed for **3a–b** and **3d–f**, is probably due to protonation of the basic N atom of the oxime group, which is occupied by the platinum center in **3a–b** and **3d–f**.

In the IR spectra of **3c–g**, we observed from one to three weak-medium to medium bands in the region of 3420–3295 cm^{-1}, which can be attributed to the N–H stretches, and a set of weak to medium bands at 3013–2870 cm^{-1} assignable to the C–H stretches.[18] All spectra also display one weak to medium band in the 1638–1597 cm^{-1} region assigned to the ν(C=N) of the amidoximate moiety[13] and one strong to very strong band at 1130–1126 cm^{-1} characteristic of the ν(S=O) of sulfur-bound sulfoxides.[19] In addition, the spectrum of **4f** displays two strong bands at 1516 and 1341 cm^{-1} specific for asymmetric and symmetric N=O stretches of the NO_2 moiety.[18]

Complexes **3c–g** are soluble in the most common deuterated organic solvents, but in $(CD_3)_2SO$, the exchange of ligated $(CH_3)_2SO$ with the solvent molecules was observed for 15 min and therefore their ^{1}H NMR spectra were recorded in $CDCl_3$. A characteristic feature of the ^{1}H NMR spectra is the availability of a singlet flanked with satellites (J_{PtH}^2 = 88–112 Hz) in the region 5.52–4.85 ppm assignable to the amide H. Another characteristic feature is the presence of two singlets with satellites (J_{PtH}^3 = 12–24 Hz) related to two Me_2SO ligands.

The ^{13}C{^{1}H} NMR spectra in $CDCl_3$ (**4c–e** and **4g**) exhibit a low-field signal at 168.94–159.19 ppm, which is attributed to the HN–*C*=NO carbon of the amidoximate moiety,[13] whereas in the high-field, the spectra display two singlets flanked with satellites (**4c–e:** J_{PtC}^2 = 32–39 Hz; **4g:** not observable due to low solubility) attributed to the methyl groups of the Me_2SO ligand at 47.02–46.96 and 46.39–46.23 ppm. Compound **4f** exhibits poor solubility in $CDCl_3$ and in other common deuterated solvents leading to a poor-quality ^{13}C{^{1}H} NMR spectrum for 12 h acquisition and it was characterized by solid-state CP-MAS TOSS ^{13}C{^{1}H} NMR. The spectrum of **4f** displays three characteristic singlets at 161.75, 45.47, and 41.01 ppm assignable to the HN–*C*=NO carbon and two O=S(*C*H$_3$)$_2$ carbons.

X-ray structure determinations

The molecular structures of **3a–b**, **3d**·MeOH, **3e–f**, **4c**, and **4f** indicate that all coordination polyhedra exhibit typical square-planar geometries (Fig. 3). In the structures of **3a–b**, **3d**·MeOH, and **3e–f**, all bond angles around the Pt^{II} centers are close to 90°, whereas the structure of **4c** and **4f** display the O(1)–Pt(1)–N(2) angles that fall into the interval 79.95–80.58°. Distortion of these angles is probably due to the chelation of the amidoximate ligands. The Pt–Cl [2.2969(9)–2.3301(17) Å] and Pt–S [2.2025(16)–2.2426(13) Å] distances exhibit values characteristic of usual Pt^{II}–Cl and Pt^{II}–S bonds.[20] The Pt(1)–N(1) bonds are in the range of 2.008(5)–2.020(3) Å, which is typical for Pt–N$_{amidoxime}$ species.[21] The S–O bond lengths [1.469(4)–1.487(5) Å] are characteristic of the sulfinyl groups of S-bound sulfoxides.[22]

In amidoxime and amidoximate ligands of **3a–b**, **3d**·MeOH, **3e–f**, **4c**, and **4f**, the O(1)–N(1), N(1)–C(1), and N(2)–C(1) distances are equal to 1.38(2)–1.437(6), 1.289(8)–1.309(4), and 1.326(5)–1.365(8) Å, respectively, and these values are specific for amidoxime and amidoximate complexes.[13] The inspection of bond length values indicate that O(1)–N(1) is a single bond,[18] whereas the N(1)–C(1) and N(2)–C(1) bonds have transitive orders between single and double bonds, but the former is rather a double bond and the latter has more single bond character.[18]

Owing to steric reasons, in **3d**·MeOH and **3e–f**, the torsion angles between the aromatic rings and the carbamidoxime moiety are in the range of 49.76–54.92°, which indicates partial delocalization between these two groups. In **4f**, the torsion angles between the groups in two crystallographically independent types of molecules are 15.60 and 22.04° favoring π-conjugation. In **3d**·MeOH and **3e–f**, one of the methyl groups of the ligated Me_2SO is located above a plane of the aromatic rings with the C$_6$···C(4) distances equal 3.642(4)–3.716(5) Å, which lead to a high-field shift of the CH_3 signals in the ^{1}H NMR spectra.

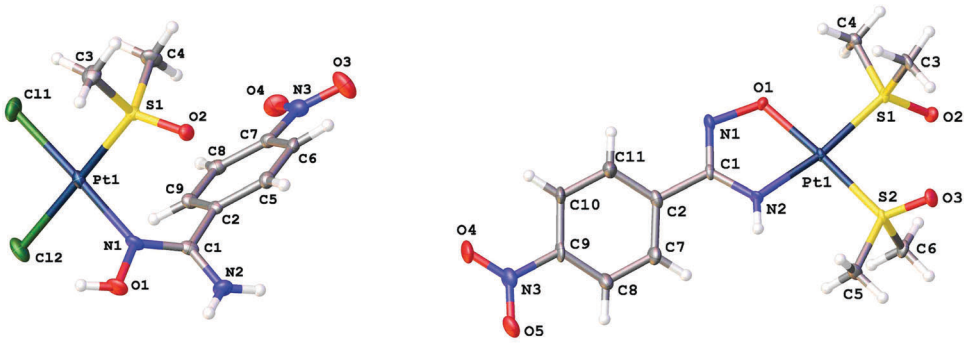

Fig. 3 Molecular structures of **3f** (left) and **4f** (right) showing the atomic numbering scheme. Thermal ellipsoids are given at the 50% probability level.

The crystal structures of **3a–b** and **3e–f** display intermolecular H-bonds between the oxygen atom of the Me_2SO ligand and one of the amide hydrogen atoms [O(2)···N(2) 2.914–2.961 Å; O(2)···H–N(2) 139.71–152.21°]. In addition, in **3a** an intermolecular H-bond was observed between the Cl(1) ligand and the HO moiety of the amidoxime ligand [Cl(1)···O(1) 3.117 Å; Cl(1)···H–O(1) 174.01°], whereas an intermolecular H-bond between the O atom of the Me_2SO ligand and the HO moiety of the amidoxime ligand was found in **3b** [O(1)···O(2) 2.749 Å; O(1)–H···O(2) 171.62°]. In **3d**·MeOH, three intermolecular H-bonds were observed, *viz.* O(1)–H···O(3) [O(1)···O(3) 2.664 Å; O(1)–H···O(3) 176.31°], N(2)–H···O(3) [N(2)···O(3) 2.975 Å; N(2)–H···O(3) 162.83°], and O(3)–H···O(2) [O(3)···O(2) 2.765 Å; O(3)–H···O(2) 161.44°].

Scope and limitations of the reactions

^{1}H NMR monitoring of the reaction between **2c** and **1** in CD_3OD at RT or 65 °C indicates that the reaction initially (the first 5 min) leads to the formation of at least four unidentified compounds, which, in particular, degrade for 24 h giving a broad mixture of products. Slow evaporation of the reaction mixture gave several crystals of $\{^tBuC(NH_2)=N(H)OH\}[PtCl_3(Me_2SO)]$, whereas the main part is an oily residue. The structure of the mono-sulfoxide complex was verified by single-crystal X-ray diffraction (see Table S2 in the ESI†). A plausible explanation of these observations is steric hindrances provided by the *tert*-butyl substituent at the oxime N atom preventing the coordination of **2c** to the platinum(II) center.

^{1}H NMR monitoring of the reaction between **2g** and **1** in CD_3OD at RT or 65 °C indicates the formation of a broad spectrum of unidentified products. In the HRESI$^+$-MS spectra, sets of peaks associated with **3g** (503.9614 $[M + Na]^+$, calcd 503.9626; 926.9742 $[2M - Cl]^+$, calcd 926.9782; 984.9367 $[2M + Na]^+$, calcd 984.9363) were found, but all these peaks could also be due to the isomeric $[PtCl_2(Me_2SO)\{NC_5H_4C(NH_2)=NOH\}]$; the coordination mode of the amidoxime ligand is typical for 4-pyridyl carbamidoxime.[13] Owing to the similar solubilities of the compounds in the mixture and their decomposition on silica gel, no pure components were isolated. We associate the formation of the mixture of products with the availability of an additional nucleophilic center, *i.e.* the pyridyl N atom, which competes with the amidoxime N atom in coordination to the metal center and provides some side-reactions.

No formation of the bis-amidoxime complexes $[PtCl_2\{RC(NH_2)=NOH\}_2]$ or $[PtCl\{RC(NH_2)=NOH\}_2(Me_2SO)]Cl$ was detected even in the presence of 10-fold excess of any one of the amidoximes **2a–g** relative to **1** in MeOH at RT or at 65 °C for 10 d. Under these conditions, only the formation of **3a–b** and **3d–f** was detected and these complexes were isolated in 70–85% yields and no sets of peaks related to the bis-amidoxime complexes were observed in HRESI$^+$-MS spectra. In addition, all attempts of the generation of $[PtCl\{RC(NH_2)=NOH\}_2(Me_2SO)](OTf)$ by treatment of **3a–b** or **3d–f** with 1 equiv. of AgOTf in MeOH from −20 to 65 °C were unsuccessful due to the formation of broad mixtures of products that we failed to separate.

The amidoximes featuring strong donor substituents R (R = 4-morpholyl, *p*-$Me_2NC_6H_4$, and *p*-$MeOC_6H_4$) react with **1** at various temperatures in the range from 0 to 65 °C in MeOH, Me_2CO, and $CHCl_3$ giving a broad spectrum of unidentified products and they could not be utilized in the reactions described above.

Comparative studies of cytotoxic activity

The antiproliferative activity of six complexes was studied *in vitro* in four human cancer cell lines by means of the colorimetric MTT assay. Species featuring the chelating amidoximate ligand (**4c–e**) exhibit higher cytotoxicity in all investigated cell lines compared to their open-chain amidoxime analogues (**3b**, **3d–e**) (Table 1).

Complexes **3b** and **3d–e** display very low activity in these cell lines with IC_{50} values consistently exceeding 100 μM and are hence about two orders of magnitude less active than the prototypic oxime complex *cis*-$[PtCl_2(Me_2C=NOH)_2]$ containing two acetoxime ligands in CH1/PA-1 and SW480 cells.[23] In contrast, most IC_{50} values of chelate congeners **4c–e** (except for A549 cells) are in the low micromolar to submicromolar range and hence at least one order of magnitude lower than those of the former complexes. In particular, complex **4e** bearing a *p*-trifluoromethylbenzamidoximate ligand shows by far the highest cytotoxic potency and displays a remarkable activity in the inherently cisplatin resistant SW480 cell line (0.51 μM *vs.* 3.3 μM, Table 1). This indicates that the trifluoromethyl substituent in the *para* position, which differentiates **4e** from **4d** (bearing an unsubstituted phenyl group), is highly favorable for cytotoxicity, enhancing it by another order of magnitude in CH1/PA-1 and SW480 cells, whereas no such effect could be observed for **3e** in comparison to **3d**.

The results for both classes of complexes are surprising, insofar as the presence of two readily exchangeable chlorido ligands in the *cis* position is not associated with high cytotoxicity here, whereas the lack of easily exchangeable ligands is. An opposite relationship between the activity of the chelate and open-chain forms was in fact previously shown for the sister class of platinum(II) compounds featuring 1,3-dihydroxyacetone oxime ligands.[10c] In contrast, one of the open-chain and not a chelate species had been shown to overcome the resistance of SW480 cells to cisplatin. It has to be borne in mind, however, that the two classes studied here are no such close analogs that can be converted into each other by (de)protonation and chloride subtraction/addition, but additionally differ by the presence of a second dimethyl sulfoxide instead of a chlorido ligand in the amidoximato complexes. In line with current knowledge on platinum drugs, it is reasonable to assume that

Table 1 Inhibition of cancer cell growth by the studied compounds; IC_{50} values (means ± SD) in four human cancer cell lines were obtained by the MTT assay (exposure time: 96 h)

	IC_{50} (μM)			
No.	CH1/PA-1	SW480	A549	SK-BR-3
3b	130 ± 44	>320	>320	202 ± 103
3d	150 ± 37	272 ± 72	>320	240 ± 78
3e	129 ± 26	157 ± 30	>320	227 ± 21
4c	19 ± 5	19 ± 4	99 ± 7	18 ± 2
4d	11 ± 1	7.9 ± 0.4	78 ± 6	13 ± 1
4e	0.96 ± 0.25	0.51 ± 0.13	30 ± 4	2.3 ± 0.3
Cisplatin[a]	0.14 ± 0.3	3.3 ± 0.4	1.3 ± 0.4	—

[a] Data taken from ref. 10*b*.

opening of the chelates is a prerequisite for high biological activity of the amidoximato complexes and that this opening may be favored by *trans* effects exerted by the sulfur donors destabilizing the opposite bonds.

These results are intriguing in the light of the known impact of dimethyl sulfoxide on the biological activity of platinum compounds. When used as a solvent for cisplatin or carboplatin (both having two chlorido ligands), $(CH_3)_2SO$ causes a profound deactivation of the drug due to ligand exchange reactions, whereas the activity of oxaliplatin (having a chelating oxalate as a leaving group) remains virtually unaffected or is slightly enhanced for unknown reasons.[19] A report on the antiproliferative activity of platinum(II) complexes of the type $[PtL_2(Me_2\underline{S}O)_2]$ (where L_2 is a chelating ligand or L is a monodentate ligand) against a set of human cancer cell lines clearly indicates low activity of these complexes relative to non-dimethyl sulfoxide analogs.[24] On the other hand, $(CH_3)_2SO$ ligands are supposed to favor the cellular uptake of metal complexes, and the increase in activity of **4c–e** might therefore also arise from the additional $(CH_3)_2SO$ ligand in this group, which may enhance the permeability of the drugs through lipid membranes.[25]

Final remarks

The possibility of pH-dependent highly selective generation of the open-chain amidoxime and chelated amidoximate platinum(II) complexes, *cis*-$[PtCl_2\{RC(NH_2)=\underline{N}OH\}(Me_2\underline{S}O)]$ and $[Pt\{RC(\underline{N}H)=NO\}(Me_2\underline{S}O)_2]$, respectively, has been demonstrated. Although the coordination chemistry of amidoximes has been extensively studied,[13] only one example of coordination isomerism of amidoximes in mononuclear complexes has previously been known, *viz.* the UO_2^{2+} center, amidoximes exhibited κ^1-*O*[26] and κ^2-*O*,N_{oxime}[27] coordination modes in neutral and basic media, respectively.

The cytotoxic properties of the novel complexes of both types were examined in four human cancer cell lines (CH1/PA-1, SW480, A549, and SK-BR-3). It was found that chelate amidoximate complexes are significantly more cytotoxic than the open-chain species. Notably, complex **4e** displays appreciably enhanced cytotoxicity in the intrinsically cisplatin-resistant SW480 cell line as compared to cisplatin, indicating a promising potential to overcome at least some forms of cisplatin resistance.

Further development of selective preparation of amidoxime complexes of other metals and studies of the cytotoxic activity of complexes featured ligands that structurally similar to amidoximes (amidrazones and hydroxamic acids) are underway in our group.

Experimental section

Materials and instrumentation

Solvents were obtained from commercial sources and used as received. Amidoximes **2a–g** were synthesized accordingly to the literature methods.[28] Melting points were measured on a Stuart SMP30 apparatus in capillaries and not corrected. Microanalyses (C, H, N) were carried out on a Euro EA3028-HT instrument. Electrospray ionization mass-spectra were obtained on a Bruker micrOTOF spectrometer equipped with an electrospray ionization (ESI) source. The instrument was operated both in negative and positive ion modes over a *m*/*z* range 50–3000. The nebulizer gas flow was 0.4 bar and the drying gas flow was 4.0 L min^{-1}. For HRESI, complexes were dissolved in MeOH. In the isotopic pattern, the most intensive peak is reported. Infrared spectra (4000–400 cm^{-1}) were recorded on a Shimadzu IR Prestige-21 instrument in KBr pellets. ^1H and $^{13}C\{^1H\}$ NMR spectra were measured on Bruker Avance 400 and Bruker Avance III 500 spectrometers at 294–298 K; residual solvent signals were used as the internal standard. The solid-state CP-MAS TOSS $^{13}C\{^1H\}$ NMR spectra were measured on a Bruker Avance III WB 400 with magic angle spinning at 6 kHz frequency.

X-Ray structure determinations

XRD experiments were carried out using Agilent Technologies "Xcalibur" (for **3a–b**, **3d**·MeOH, **3e–f**, and **4c**) and "Supernova" (for **4f**) diffractometers with monochromated MoKα or CuKα radiation, respectively. Crystals were fixed on a micro mount, placed on diffractometer and measured at a temperature of 100 K. The unit cell parameters (Tables S1 and S2, ESI†) were refined by least square techniques in the 2θ range of 5.6–55.0 for MoKα and 9.0–150.0 for CuKα. The structures have been solved using the Superflip[29] structure solution program using charge flipping and refined with the ShElXL[30] refinement incorporated in the *OLEX2* program package.[31] The carbon-bound H atoms were placed in calculated positions and included in the refinement in the 'riding' model approximation, with $U_{iso}(H)$ set to $1.2U_{eq}(C)$ and C–H 0.97 Å for the CH_2 groups, $U_{iso}(H)$ set to $1.5U_{eq}(C)$ and C–H 0.96 Å for the CH_3 groups, $U_{iso}(H)$ set to $1.2U_{eq}(C)$ and C–H 0.93 Å for the CH groups, $U_{iso}(H)$ set to $1.2U_{eq}(N)$ and N–H 0.88 Å for the NH and NH_2 groups and $U_{iso}(H)$ set to $1.5U_{eq}(O)$ and O–H 0.82 Å for the OH groups. Empirical absorption correction was applied in the CrysAlisPro[32] program complex using spherical harmonics (for **3a–b**, **3d**·MeOH, **3e–f**, and **4c**), implemented in the SCALE3 ABSPACK scaling algorithm. For **4f**, numerical absorption correction based on Gaussian integration over a multifaceted crystal model was applied (Tables S1 and S2, ESI†).

Cell lines and culture conditions

The cytotoxicity tests were performed in four human cancer cell lines. CH1/PA-1 cells (identified *via* STR profiling as PA-1 ovarian teratocarcinoma cells by Multiplexion, Heidelberg, Germany; compare ref. 33) were kindly provided by Lloyd R. Kelland (CRC Centre for Cancer Therapeutics, Institute of Cancer Research, Sutton, UK). SW480 (human adenocarcinoma of the colon) and A549 (human non-small cell lung cancer) cells were obtained from Brigitte Marian (Institute of Cancer Research, Department of Medicine I, Medical University of Vienna, Austria) and SK-BR-3 (human adenocarcinoma of the mammary gland) cells from Evelyn Dittrich (General Hospital, Medical University of Vienna, Austria). Cell monolayer adherent cultures were grown in 75 cm^2 culture flasks (Starlab, Germany) in complete medium [*i.e.*, minimal essential medium (MEM) supplemented with 10% heat-inactivated fetal bovine serum

(Life Technologies, Germany), 1% sodium pyruvate, 1% non-essential amino acids from 100× ready-to-use stock and 2% L-glutamine (all purchased from Sigma-Aldrich, Austria)]. Cell cultures were incubated at 37 °C in a moist atmosphere containing 5% CO_2 in air.

Cytotoxicity tests in cancer cell lines

The cytotoxic activity *in vitro* was determined by means of the colorimetric microculture MTT assay (MTT = 3-(4,5-dimethyl-2-thiazolyl)-2,5-diphenyl-2*H*-tetrazolium bromide). For this purpose, cells were harvested from culture flasks by trypsinization and seeded into 96-well plates (Starlab, Germany) at densities of 1.25×10^3 cells per well (CH1/PA-1), 2×10^3 cells per well (SW480), 3×10^3 cells per well (A549) and 5×10^3 cells per well (SK-BR-3) in volumes of 100 μL per well. Cells were allowed to settle and proliferate for 24 h before exposure to the drugs. Stock solutions of each complex were prepared in $(CH_3)_2SO$, appropriately diluted in complete medium (not to exceed a concentration of 0.5% $(CH_3)_2SO$ in cells) and instantly added into the plates (100 μL per well). After continuous exposure for 96 h, drug solutions were replaced with 100 μL per well of a 1 : 6 MTT/RPMI 1640 solution (MTT solution, 5 mg mL^{-1} of MTT reagent in phosphate-buffered saline; RPMI 1640 medium, supplemented with 10% heat-inactivated fetal bovine serum and 2% L-glutamine). After incubation for 4 h, the medium/MTT mixtures were removed, and the formazan crystals formed by viable cells were dissolved in $(CH_3)_2SO$ (150 μL per well). Optical densities were measured at 550 nm using a microplate reader (ELx808 Absorbance Microplate Reader, Bio-Tek, USA), using a reference wavelength of 690 nm to correct for unspecific absorption. The quantity of viable cells was expressed in relation to the untreated control and 50% inhibitory concentrations (IC_{50}) were calculated from concentration–effect curves by interpolation. Evaluation is based on means from at least three independent experiments, each comprising triplicates per concentration level.

Synthetic work

Preparation of amidoxime complexes 3a–b and 3d–f

Powder of *cis*-[$PtCl_2(Me_2SO)_2$] (**1**) (84.5 mg; 200 μmol) was added into a stirred solution of any one of the amidoximes **2a–b** and **2d–f** (200 μmol) in MeOH (3 mL). The suspension was left to stand at 65 °C under stirring for 5 min, whereupon the homogeneous solution formed was cooled to RT and the solvent was evaporated at RT *in vacuo*. The oily residue was crystallized under $CHCl_3$ (1 mL) and separated by centrifugation. The precipitate was washed with two 1.5 mL portions of Et_2O and dried in air at 65 °C. For the characterization of **3a–b** and **3d–e**, see the ESI.†

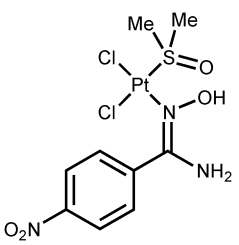

3f. Yield: 98% (102.9 mg). Mp: 183 °C (dec). Anal. calcd for $C_9H_{13}N_3Cl_2O_4PtS$: C, 21.65; H, 3.52; N, 6.39. Found: C, 21.73; H, 3.41; N, 6.48. HRESI$^+$-MS (MeOH, *m*/*z*): 453.0172 ([M − 2Cl − H]$^+$, calcd 453.0191), 489.9923 ([M − Cl]$^+$, calcd 489.9946), 547.9517 ([M + Na]$^+$, calcd 547.9524), 1014.9577 ([2M − Cl]$^+$, calcd 1014.9580), 1072.9157 ([2M + Na]$^+$, calcd 1072.9161). IR (KBr, selected bonds, cm^{-1}): 3439(s), 3335(s) ν(O–H) and ν(N–H); 3185(m), 3107(w), 3079(w), 3001(w-m), 2918(w-m) ν(C–H); 1661(vs) ν(C═N); 1520(vs) $\nu(N{=}O)_{as}$; 1346(vs) $\nu(N{=}O)_s$; 1136(s) ν(S═O). ^{1}H NMR (CD_3OD, δ): 8.43 (d, 2H, C*H*), 8.19 (d, 2H, C*H*), 3.42 (s, 3H, CH_3), 2.83 (s, 3H, CH_3). CP-MAS TOSS $^{13}C\{^1H\}$ NMR (δ): 155.19 ($C(NH_2){=}NOH$), 149.60, 148.08, 146.40, 138.11, 133.02, 129.73, 123.36, 122.12 (Ar), 46.59, 44.17, 42.66, 40.18 (s, CH_3). Crystals of **3f** suitable for X-ray diffraction were obtained by slow evaporation of $MeNO_2$ solution at RT in air.

Preparation of amidoximate complexes 4c–g

Powder of *cis*-[$PtCl_2(Me_2SO)_2$] (**1**) (84.5 mg; 200 μmol) was added into a stirred solution of any of the amidoximes **2a–g** (200 μmol) and NaOH (20.0 mg; 500 μmol) in MeOH (3 mL). The suspension was left to stand at 65 °C under stirring for 20 min, whereupon the suspension formed was cooled to RT and the solvent was evaporated at RT *in vacuo*. The solid obtained was washed by one 0.5 mL portion of cold (−20 °C) MeOH and two 1.5 mL portions of Et_2O, and dried in air at 65 °C. For the characterization of **4c–e** and **4g**, see the ESI.†

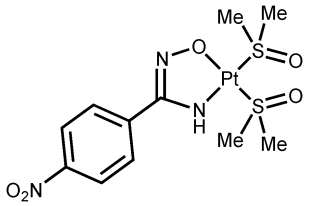

4f·H_2O. Yield: 95% (104.1 mg). Mp: 210 °C (dec). Anal. calcd for $C_{11}H_{17}N_3O_5PtS_2{\cdot}H_2O$: C, 24.09; H, 3.49; N, 7.66. Found: C, 23.99; H, 3.54; N, 7.65. HRESI$^+$-MS (*m*/*z*): 531.0306 ([M + H]$^+$, calcd 531.0331), 553.0104 ([M + Na]$^+$, calcd 553.0150). IR (KBr, selected bonds, cm^{-1}): 3414(m), 3335(m) ν(N–H); 2990(m), 2913(m) ν(C–H); 1597(m) ν(C═N); 1516(m-s) $\nu(N{=}O)_{as}$; 1341(s) $\nu(N{=}O)_s$; 1130(vs) ν(S═O). ^{1}H NMR ($CDCl_3$, δ): 8.20 (d, 2H, C*H*), 7.92 (d, 2H, C*H*), 5.27 (s + d, $J_{PtH}{}^2$ = 108 Hz, br, 1H, N*H*), 3.58 (s + d, $J_{PtH}{}^3$ = 20 Hz, 6H, $S(CH_3)_2$), 3.55 (s + d, $J_{PtH}{}^3$ = 20 Hz, 6H, $S(CH_3)_2$). CP-MAS TOSS $^{13}C\{^1H\}$ NMR ($CDCl_3$, δ): 161.75 ($C(NH){=}NO$), 148.61, 145.56, 135.64, 123.33 (Ar), 45.47 ($S(CH_3)_2$), 41.01 ($S(CH_3)_2$). Crystals of **4f** suitable for X-ray diffraction were obtained by slow evaporation of MeOH solution at RT in air.

Acknowledgements

The authors are grateful to the Russian Foundation for Basic Research (project 16-03-00573), the Scientific Council of the President of the Russian Federation (project MK-473.2017.3), and RAS (program 1.14P) for financial support. Physicochemical

studies were performed at the Magnetic Resonance Research Center, Center for X-ray Diffraction Studies, Center for Chemical Analysis and Materials Research, and Chemistry Educational Center of Saint Petersburg State University.

References

1 (*a*) A. V. Klein and T. W. Hambley, *Ligand Design in Medicinal Inorganic Chemistry*, John Wiley & Sons, Ltd., 2014, pp. 9–45; (*b*) S. Dilruba and G. V. Kalayda, *Cancer Chemother. Pharmacol.*, 2016, **77**, 1103–1124; (*c*) N. J. Wheate, S. Walker, G. E. Craig and R. Oun, *Dalton Trans.*, 2010, **39**, 8113–8127.

2 S. H. van Rijt and P. J. Sadler, *Drug Discovery Today*, 2009, **14**, 1089–1097.

3 (*a*) T. Boulikas, A. Pantos, E. Bellis and P. Christofis, *Anti-cancer Therapeutics*, John Wiley & Sons, Ltd., 2008, pp. 55–78; (*b*) J. Zhang, Y. Ke and J. Shen, *Shanghai Yiyao*, 2013, **34**, 52–59; (*c*) M. G. Apps, E. H. Y. Choi and N. J. Wheate, *Endocr.-Relat. Cancer*, 2015, **22**, R219–R233.

4 M. A. Jakupec, M. Galanski, V. B. Arion, C. G. Hartinger and B. K. Keppler, *Dalton Trans.*, 2008, 183–194.

5 (*a*) V. Brabec and J. Kasparkova, *Metal Compounds in Cancer Chemotherapy*, Research Signpost, 2005, pp. 187–218; (*b*) D. Wang and S. J. Lippard, *Nat. Rev. Drug Discovery*, 2005, **4**, 307–320; (*c*) S. Ahmad, A. A. Isab and S. Ali, *Transition Met. Chem.*, 2006, **31**, 1003–1016; (*d*) S. J. Berners-Price, L. Ronconi and P. J. Sadler, *Prog. Nucl. Magn. Reson. Spectrosc.*, 2006, **49**, 65–98; (*e*) M. J. Hannon, *Pure Appl. Chem.*, 2007, **79**, 2243–2261; (*f*) B. Wu, G. E. Davey, A. A. Nazarov, P. J. Dyson and C. A. Davey, *Nucleic Acids Res.*, 2011, **39**, 8200–8212; (*g*) J. J. Wilson and S. J. Lippard, *Chem. Rev.*, 2014, **114**, 4470–4495.

6 (*a*) F. Arnesano, A. Pannunzio, M. Coluccia and G. Natile, *Coord. Chem. Rev.*, 2015, **284**, 286–297; (*b*) X. Wang, X. Wang and Z. Guo, *Acc. Chem. Res.*, 2015, **48**, 2622–2631; (*c*) J. Pracharova, T. Radosova Muchova, E. Dvorak Tomastikova, F. P. Intini, C. Pacifico, G. Natile, J. Kasparkova and V. Brabec, *Dalton Trans.*, 2016, **45**, 13179–13186.

7 (*a*) A. D. Ryabov, *Ross. Khim. Zh.*, 1996, **40**, 33–42; (*b*) A. S. de Pascali, A. Muscella, S. Marsigliante, M. G. Bottone, G. Bernocchi and F. P. Fanizzi, *Pure Appl. Chem.*, 2013, **85**, 355–364; (*c*) F.-U. Rahman, A. Ali, R. Guo, Y.-C. Zhang, H. Wang, Z.-T. Li and D.-W. Zhang, *Dalton Trans.*, 2015, **44**, 2166–2175; (*d*) M. Serratrice, L. Maiore, A. Zucca, S. Stoccoro, I. Landini, E. Mini, L. Massai, G. Ferraro, A. Merlino, L. Messori and M. A. Cinellu, *Dalton Trans.*, 2016, **45**, 579–590; (*e*) C. M. A. Müller, M. V. Babak, M. Kubanik, M. Hanif, S. M. F. Jamieson, C. G. Hartinger and L. J. Wright, *Inorg. Chim. Acta*, 2016, **450**, 124–130.

8 (*a*) E. Alessio, G. Mestroni, A. Bergamo and G. Sava, *Curr. Top. Med. Chem.*, 2004, **4**, 1525–1535; (*b*) C. G. Hartinger, S. Zorbas-Seifried, M. A. Jakupec, B. Kynast, H. Zorbas and B. K. Keppler, *J. Inorg. Biochem.*, 2006, **100**, 891–904; (*c*) A. Bergamo and G. Sava, *Dalton Trans.*, 2007, 1267–1272; (*d*) I. Bratsos, S. Jedner, T. Gianferrara and E. Alessio, *Chimia*, 2007, **61**, 692–697; (*e*) A. Bergamo, C. Gaiddon, J. H. M. Schellens, J. H. Beijnen and G. Sava, *J. Inorg. Biochem.*, 2012, **106**, 90–99; (*f*) S. Pillozzi, L. Gasparoli, M. Stefanini, M. Ristori, M. D'Amico, E. Alessio, F. Scaletti, A. Becchetti, A. Arcangeli and L. Messori, *Dalton Trans.*, 2014, **43**, 12150–12155; (*g*) S. Komeda and A. Casini, *Curr. Top. Med. Chem.*, 2012, **12**, 219–235; (*h*) S. Leijen, S. A. Burgers, P. Baas, D. Pluim, M. Tibben, E. van Werkhoven, E. Alessio, G. Sava, J. H. Beijnen and J. H. M. Schellens, *Invest. New Drugs*, 2015, **33**, 201–214.

9 (*a*) N. Farrell, *Cancer Invest.*, 1993, **11**, 578–589; (*b*) N. P. Farrell, *Chem. Soc. Rev.*, 2015, **44**, 8773–8785; (*c*) T. C. Johnstone, S. J. Lippard and K. Suntharalingam, *Chem. Rev.*, 2016, **116**, 3436–3486.

10 (*a*) Y. Y. Scaffidi-Domianello, K. Meelich, M. A. Jakupec, V. B. Arion, V. Y. Kukushkin, M. Galanski and B. K. Keppler, *Inorg. Chem.*, 2010, **49**, 5669–5678; (*b*) Y. Y. Scaffidi-Domianello, A. A. Legin, M. A. Jakupec, A. Roller, V. Y. Kukushkin, M. Galanski and B. K. Keppler, *Inorg. Chem.*, 2012, **51**, 7153–7163; (*c*) Y. Y. Scaffidi-Domianello, A. A. Legin, M. A. Jakupec, V. B. Arion, V. Y. Kukushkin, M. Galanski and B. K. Keppler, *Inorg. Chem.*, 2011, **50**, 10673–10681; (*d*) D. A. Erdogan and S. Ozalp-Yaman, *J. Mol. Struct.*, 2014, **1064**, 50–57; (*e*) K. Ossipov, Y. Y. Scaffidi-Domianello, I. F. Seregina, M. Galanski, B. K. Keppler, A. R. Timerbaev and M. A. Bolshov, *J. Inorg. Biochem.*, 2014, **137**, 40–45; (*f*) Y. Benabdelouahab, L. Munoz-Moreno, M. Frik, I. de la Cueva-Alique, M. A. El Amrani, M. Contel, A. M. Bajo, T. Cuenca and E. Royo, *Eur. J. Inorg. Chem.*, 2015, 2295–2307; (*g*) H. Meyer, M. Brenner, S.-P. Hoefert, T.-O. Knedel, P. C. Kunz, A. M. Schmidt, A. Hamacher, M. U. Kassack and C. Janiak, *Dalton Trans.*, 2016, **45**, 7605–7615; (*h*) M. Kubanik, W. Kandioller, K. Kim, R. F. Anderson, E. Klapproth, M. A. Jakupec, A. Roller, T. Sohnel, B. K. Keppler and C. G. Hartinger, *Dalton Trans.*, 2016, **45**, 13091–13103.

11 (*a*) I. Racz, K. Tory, F. J. Gallyas, Z. Berente, E. Osz, L. Jaszlits, S. Bernath, B. Sumegi, G. Rabloczky and P. Literati-Nagy, *Biochem. Pharmacol.*, 2002, **63**, 1099–1111; (*b*) T. Kardon, G. Nagy, M. Csala, A. Kiss, Z. Schaff, P. L. Nagy, L. Wunderlich, G. Banhegyi and J. Mandl, *Anticancer Res.*, 2006, **26**, 1023–1028; (*c*) K. C. Fylaktakidou, D. J. Hadjipavlou-Litina, K. E. Litinas, E. A. Varella and D. N. Nicolaides, *Curr. Pharm. Des.*, 2008, **14**, 1001–1047.

12 (*a*) D. S. Bolotin, A. S. Novikov, I. E. Kolesnikov, V. V. Suslonov, Y. Novozhilov, O. Ronzhina, M. Dorogov, M. Krasavin and V. Y. Kukushkin, *ChemistrySelect*, 2016, **1**, 456–461; (*b*) Y. Kaya, C. Icsel, V. T. Yilmaz and O. Buyukgungor, *J. Mol. Struct.*, 2015, **1095**, 51–60; (*c*) E. Y. Bulatov, T. G. Chulkova, I. A. Boyarskaya, V. V. Kondratiev, M. Haukka and V. Y. Kukushkin, *J. Mol. Struct.*, 2014, **1068**, 176–181.

13 D. S. Bolotin, N. A. Bokach and V. Y. Kukushkin, *Coord. Chem. Rev.*, 2016, **313**, 62–93.

14 (*a*) A. B. Goel, S. Goel and D. Vanderveer, *Inorg. Chim. Acta*, 1981, **54**, L5–L6; (*b*) A. D. Ryabov, G. M. Kazankov, I. M. Panyashkina, O. V. Grozovsky, O. G. Dyachenko,

V. A. Polyakov and L. G. Kuz'mina, *Dalton Trans.*, 1997, 4385–4391; (*c*) T. Kluge, M. Bette, T. Rüffer, C. Bruhn, C. Wagner, D. Ströhl, J. Schmidt and D. Steinborn, *Organometallics*, 2013, **32**, 7090–7106.

15 N. Dürüst, M. A. Akay, Y. Dürüst and E. Kiliç, *Anal. Sci.*, 2000, **16**, 825–827.

16 (*a*) V. Y. Kukushkin, A. J. L. Pombeiro, C. M. P. Ferreira, L. I. Elding and R. J. Puddephatt, *Inorg. Synth.*, 2002, **33**, 189–196; (*b*) Y. N. Kukushkin, Y. E. Vyaz'menskii, L. I. Zorina and Y. L. Pazukhina, *Zh. Neorg. Khim.*, 1968, **13**, 1595–1599.

17 (*a*) T.-C. Chien, C.-H. Wang, T.-H. Hsieh, C.-C. Lin, W.-H. Yeh and C.-A. Lin, *Synlett*, 2015, 1823–1826; (*b*) D. S. Bolotin, K. I. Kulish, N. A. Bokach, G. L. Starova, V. V. Gurzhiy and V. Y. Kukushkin, *Inorg. Chem.*, 2014, **53**, 10312–10324.

18 L. J. Bellamy, *The infra-red spectra of complex molecules*, Methuen and co. Ltd, John Wiley and sons, Inc, London, New York, 1958.

19 E. D. Risberg, J. Mink, A. Abbasi, M. Y. Skripkin, L. Hajba, P. Lindqvist-Reis, É. Bencze and M. Sandström, *Dalton Trans.*, 2009, 1328–1338, DOI: 10.1039/b814252a.

20 A. G. Orpen, L. Brammer, F. H. Allen, O. Kennard, D. G. Watson and R. Taylor, *J. Chem. Soc., Dalton Trans.*, 1989, **12**, S1–S83.

21 (*a*) D. S. Bolotin, M. Y. Demakova, A. S. Novikov, M. S. Avdontceva, M. L. Kuznetsov, N. A. Bokach and V. Y. Kukushkin, *Inorg. Chem.*, 2015, **54**, 4039–4046; (*b*) D. S. Bolotin, N. A. Bokach, M. Haukka and V. Y. Kukushkin, *ChemPlusChem*, 2012, **77**, 31–40; (*c*) D. S. Bolotin, N. A. Bokach, M. Haukka and V. Y. Kukushkin, *Inorg. Chem.*, 2012, **51**, 5950–5964.

22 Y. Y. Scaffidi-Domianello, A. A. Nazarov, M. Haukka, M. Galanski, B. K. Keppler, J. Schneider, P. Du, R. Eisenberg and V. Y. Kukushkin, *Inorg. Chem.*, 2007, **46**, 4469–4482.

23 S. Zorbas-Seifried, M. A. Jakupec, N. V. Kukushkin, M. Groessl, C. G. Hartinger, O. Semenova, H. Zorbas, V. Y. Kukushkin and B. K. Keppler, *Mol. Pharmacol.*, 2007, **71**, 357–765.

24 (*a*) M. D. Hall, K. A. Telma, K. E. Chang, T. D. Lee, J. P. Madigan, J. R. Lloyd, I. S. Goldlust, J. D. Hoeschele and M. M. Gottesman, *Cancer Res.*, 2014, **74**, 3913–3922; (*b*) P. Bergamini, L. Marvelli, G. Spirandelli and E. Gallerani, *Inorg. Chim. Acta*, 2016, **439**, 35–42; (*c*) T. A. K. Al-Allaf, L. J. Rashan, A. S. Abu-Surrah, R. Fawzi and M. Steimann, *Transition Met. Chem.*, 1998, **23**, 403–406.

25 R. Notman, M. Noro, B. O'Malley and J. Anwar, *J. Am. Chem. Soc.*, 2006, **128**, 13982–13983.

26 E. G. Witte and K. S. Schwochau, *Inorg. Chim. Acta*, 1984, **94**, 323–331.

27 S. Vukovic, L. A. Watson, S. O. Kang, R. Custelcean and B. P. Hay, *Inorg. Chem.*, 2012, **51**, 3855–3859.

28 (*a*) J. K. Augustine, V. Akabote, S. G. Hegde and P. Alagarsamy, *J. Org. Chem.*, 2009, **74**, 5640–5643; (*b*) C. C. Lin, T. H. Hsieh, P. Y. Liao, Z. Y. Liao, C. W. Chang, Y. C. Shih, W. H. Yeh and T. C. Chien, *Org. Lett.*, 2014, **16**, 892–895.

29 (*a*) L. Palatinus and G. Chapuis, *J. Appl. Crystallogr.*, 2007, **40**, 786–790; (*b*) L. Palatinus, S. J. Prathapa and S. van Smaalen, *J. Appl. Crystallogr.*, 2012, **45**, 575–580.

30 G. M. Sheldrick, *Acta Crystallogr., Sect. C: Struct. Chem.*, 2015, **71**, 3–8.

31 O. V. Dolomanov, L. J. Bourhis, R. J. Gildea, J. A. K. Howard and H. Puschmann, *J. Appl. Crystallogr.*, 2009, **42**, 339–341.

32 CrysAlisPro, 1.171.36.20; Agilent Technologies: Santa Clara, CA, 2012.

33 C. Korch, M. A. Spillman, T. A. Jackson, B. M. Jacobsen, S. K. Murphy, B. A. Lessey, V. C. Jordan and A. P. Bradford, *Gynecol. Oncol.*, 2012, **127**, 241–248.

